Chapter- 4

Effects of magnetic field on the flow of a Jeffrey fluid through a porous medium in an annulus with peristalsis

4.1 Introduction

In recent years, the flow of non-Newtonian fluids has been an important topic in the field of biomedical and environmental engineering and science. Certainly the mechanics of non-Newtonian fluids presents special challenges to engineers, physicists, and mathematicians. This is due to the fact that nonlinearity evident itself in a variety of ways. The flow of non-Newtonian fluids is not only important because of their technological significance but also in the interesting mathematical features presented by the equations that governing the flow. Extensive literature on the subject is now available. Peristaltic transport of blood in small vessels was investigated using the viscoelastic, power-law, Casson, micropolar fluid models by (Bhome and Friedrich, [11]; Radhakrishnamacharya, 1982[47]; Srivastava and Srivastava, 1984[58]; Srinivasacharya et al., 2003[56]. Hayat et al. 2006[29] have studied the the peristaltic flow of a Jeffrey fluid assuming chyme as a non-Newtonian fluid in an annulus. The effect of an endoscope on the peristaltic flow of a micropolar fluid was studied by Hayat and Ali [32].

The study of MHD flow problems has gained considerable interest in recent years because of its extensive engineering and medical applications. The effect of moving magnetic field on blood flow was first investigated by Stud et al (1977)[61]. They observed that the effect of suitable moving magnetic field accelerates the speed of blood. Agrawal and Anwaruddin (1984)[3] have studied the effect of magnetic field on blood flow by taking a simple mathematical model for blood through an equally branched channel with flexible outer walls executing peristaltic waves. The influence of an endoscope on the peristaltic flow of a Jeffrey fluid under the effective of magnetic filed in a tube was studied by Hayat et al. (2008)[33]. Peristaltic flow of a Jeffrey fluid under the effect of a magnetic field in a tube was discussed by Hayat and Ali (2008)[32]. Furthermore, flow through a porous medium has practical applications especially in geophysical fluid dynamics. Examples of natural porous medium are beach sand, sandstone, lime stone, rye bread, wood, the human lung, bile duct, gall bladder with

stones and in small blood vessels. In view of this, El Shehawey et al. [18] investigated the peristaltic flow of a Newtonian fluid through a porous medium. Mekheimer and Al-Arabi (2003)[[40] have discussed the peristaltic flow of a Newtonian fluid through a porous medium in a channel under the effect of magnetic field. The peristaltic flow of electrically conducting fluid through a porous medium in a planar channel was investigated by Hayat et al. (2007)[29]. Sudhakar Reddy et al. (2009)[69] have studied peristaltic motion of a Carreau fluid through a porous medium in a channel under the effect of a magnetic field. Subba Reddy and Prasanth Reddy (2010)[65] have investigated the peristaltic pumping of a Jeffrey fluid with variable viscosity through a porous medium in a planar channel.

In view of these, we studied the effect of magnetic field on the peristaltic transport of a Jeffrey fluid through a porous medium in an annulus. The analysis has been carried out in the wave frame of reference with long wavelength and zero Reynolds number assumptions. The expressions for the velocity field and the heat transfer coefficient are obtained analytically. The effects of various emerging parameters on the axial pressure gradient and pumping characteristics are discussed in detail with the aid of graphs.

4.2 Mathematical Formulation

We consider the peristaltic transport of an incompressible conducting Jeffrey fluid through a porous annular region between two coaxial vertical tubes. The flow is generated by sinusoidal wave trains propagating with constant speed c along the wall of the outer tube. The fluid subjected to a constant transverse magnetic field. Induced magnetic field, external electric field, electric field due to polarization of charges, heat due to viscous and joule dissipation are neglected. The axisymmetric cylindrical polar coordinate system (Z, R) is chosen such that the Z - coordinate is along the center line of the inner and outer tubes and R - coordinate along the radial coordinate. Fig. 4.1 depicts the physical model of the problem.

The geometry of the inner and outer walls are defined by

$$R = R_1 = a_0 \qquad (4.2.1)$$

$$R = R_2(Z,t) = a + b\sin\left(\frac{2\pi}{\lambda}[Z - ct]\right) \qquad (4.2.2)$$

where a_0, a are the radii of the inner and outer tubes, b is the amplitude of the wave, λ is the wavelength and t is the time.

The flow is unsteady in the fixed frame (Z, R). However, in a co-ordinate system moving with the propagation velocity c (wave frame (z, r)), the boundary shape is stationary. The transformation from fixed frame to wave frame is given by

$$z = Z - ct, r = R, w = W - c, u = U \qquad (4.2.3)$$

where (w, u) and (W, U) are the velocity components in the wave and fixed frames respectively.

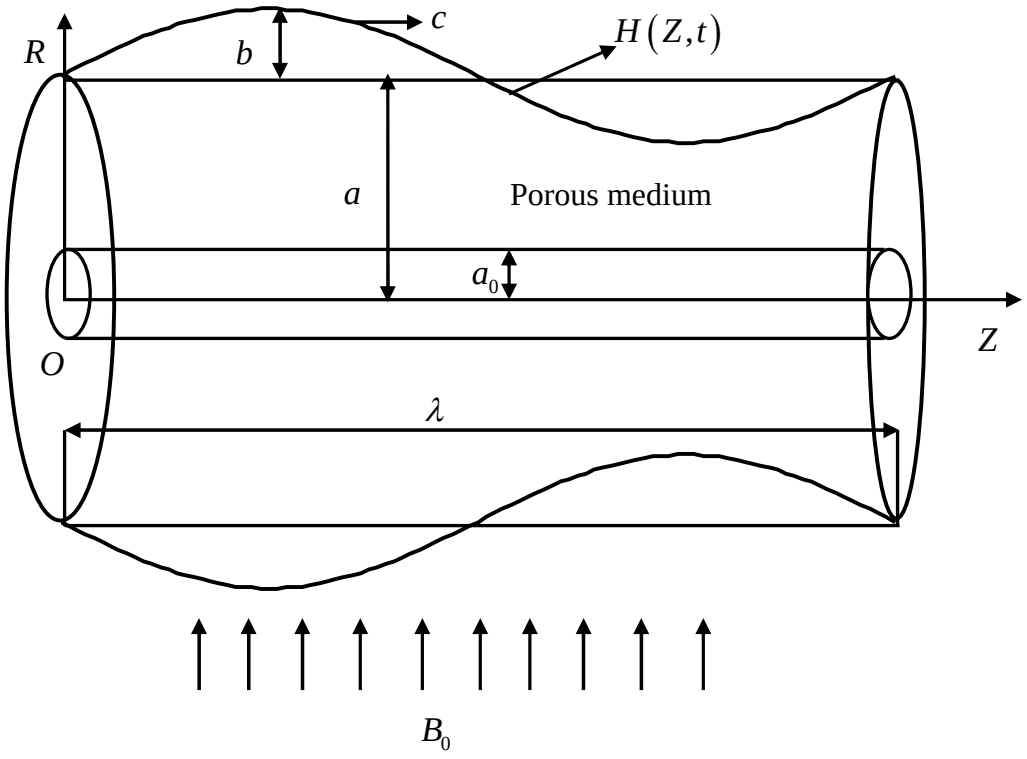

Fig. 4.1. The physical model

The constitute equation of S for Jeffrey fluid is

$$S = \frac{\mu}{1+\lambda_1}\left(\dot{\gamma} + \lambda_2 \ddot{\gamma}\right) \tag{4.2.4}$$

where μ is the dynamic viscosity, λ_1 is the ratio of relaxation to retardation times, λ_2 is the retardation time, $\dot{\gamma}$ is the shear rate and dots over the quantities denotes differentiation with time.

The equations governing the flow in the wave frame of reference are

$$\frac{\partial u}{\partial r} + \frac{u}{r} + \frac{\partial w}{\partial z} = 0 \tag{4.2.5}$$

$$\rho\left(u\frac{\partial u}{\partial r} + w\frac{\partial u}{\partial z}\right) = -\frac{\partial p}{\partial r} + \frac{1}{r}\frac{\partial}{\partial r}\left(rS_{rr}\right) + \frac{\partial S_{rz}}{\partial z} - \frac{\mu}{k}u \tag{4.2.6}$$

$$\rho\left(u\frac{\partial w}{\partial r} + w\frac{\partial w}{\partial z}\right) = -\frac{\partial p}{\partial z} + \frac{1}{r}\frac{\partial}{\partial r}(rS_{rz}) + \frac{\partial S_{zz}}{\partial z} - \left(\sigma B_0^2 + \frac{\mu}{k}\right)\left(w + c\right) \tag{4.2.7}$$

where p is the pressure, k is the permeability of the porous medium and ρ is the density of the fluid.

The dimensional boundary conditions are

$$w = -c \qquad \text{at} \qquad r = R_1, R_2(z) \tag{4.2.8}$$

Introducing the non-dimensional variables defined by

$$\bar{r} = \frac{r}{a},\ \bar{z} = \frac{z}{\lambda},\ \bar{w} = \frac{w}{c},\ \bar{u} = \frac{u}{c\delta},\ \bar{p} = \frac{pa^2}{\mu c\lambda},\ \bar{S} = \frac{aS}{\mu c},\ \ \delta = \frac{a}{\lambda},$$

$$\bar{r}_1 = \frac{r_1}{a},\ \ \bar{r}_2 = \frac{r_2}{a} = 1 + \phi\sin\left(2\pi z\right),\ \phi = \frac{b}{a},\ Da = \frac{k_0}{a^2},\ \mathrm{Re} = \frac{\rho ac}{\mu}, \tag{4.2.9}$$

where Da is the Darcy number, Re is the Reynolds number, δ is the wave number, ϕ is the amplitude ratio, into the Equations (4.2.5) – (4.2.7), we obtain (after dropping the bars)

$$\frac{\partial u}{\partial r} + \frac{u}{r} + \frac{\partial w}{\partial z} = 0 \tag{4.2.10}$$

$$\mathrm{Re}\,\delta^3\left(u\frac{\partial u}{\partial r} + w\frac{\partial u}{\partial z}\right) = -\frac{\partial p}{\partial r} + \frac{\delta}{r}\frac{\partial}{\partial r}\left(rS_{rr}\right) + \delta^2\frac{\partial S_{rz}}{\partial z} - \frac{\delta}{Da}u \tag{4.2.11}$$

$$\mathrm{Re}\,\delta\left(u\frac{\partial w}{\partial r} + w\frac{\partial w}{\partial z}\right) = -\frac{\partial p}{\partial z} + \frac{1}{r}\frac{\partial}{\partial r}(rS_{rz}) + \delta\frac{\partial S_{zz}}{\partial z} - \left(M^2 + \frac{1}{Da}\right)\left(w + 1\right) \tag{4.2.12}$$

where

$$S_{rr} = \frac{2\delta}{1+\lambda_1}\left[1+\frac{\lambda_2 c\delta}{a}\left(u\frac{\partial}{\partial r}+w\frac{\partial}{\partial z}\right)\right]\frac{\partial u}{\partial r},$$

$$S_{rz} = \frac{1}{1+\lambda_1}\left[1+\frac{\lambda_2 c\delta}{a}\left(u\frac{\partial}{\partial r}+w\frac{\partial}{\partial z}\right)\right]\left(\frac{\partial w}{\partial r}+\delta^2\frac{\partial u}{\partial z}\right),$$

and $S_{zz} = \frac{2\delta}{1+\lambda_1}\left[1+\frac{\lambda_2 c\delta}{a}\left(u\frac{\partial}{\partial r}+w\frac{\partial}{\partial z}\right)\right]\frac{\partial w}{\partial z}.$

Under lubrication approach (i.e., $\delta << 1$ and $\mathrm{Re} \to 0$), the Equations (4.2.11) and (4.2.12) become

$$\frac{\partial p}{\partial r} = 0 \tag{4.2.13}$$

$$\frac{\partial p}{\partial z} = \frac{1}{(1+\lambda_1)r}\frac{\partial}{\partial r}\left(r\frac{\partial w}{\partial r}\right)-\frac{1}{Da}(w+1) \tag{4.2.14}$$

From Eq. (4.2.13) and (4.2.14), we write Eq. (4.2.14) as

$$(1+\lambda_1)\frac{dp}{dz} = \frac{1}{r}\frac{\partial}{\partial r}\left(r\frac{\partial w}{\partial r}\right)-N^2(w+1) \tag{4.2.15}$$

here $\Omega^2 = M^2 + \frac{(1+\lambda_1)}{Da}$.

The corresponding non-dimensional boundary conditions are

$$w = -1 \qquad \text{at} \qquad r = r_1, r_2 \tag{4.2.16}$$

The dimensionless volume flow rate in the wave frame is given by

$$q = 2\int_{r_1}^{r_2} wr\,dr \tag{4.2.17}$$

The dimensionless instantaneous volume flow rate in the fixed frame of reference is given by

$$Q(z,t) = 2\int_{r_1}^{r_2} WR\,dR = 2\int_{r_1}^{r_2}(w+1)r\,dr = q + r_2^2 - r_1^2 \tag{4.2.18}$$

The dimensionless time mean flow over a period $T\left(=\lambda/c\right)$ of the peristaltic wave, is defined as

$$\overline{Q} = \frac{1}{T}\int_0^T Q(z,t)dt = q + 1 + \frac{\phi^2}{2} - r_1^2 \tag{4.2.19}$$

4.3. Solution

Solving Eq. (4.2.15) together with the boundary conditions (4.2.16), we get

$$w = \frac{(1+\lambda_1)}{\Omega^2}\frac{dp}{dz}\left[A_1 I_0(\Omega r) + A_2 K_0(\Omega r) - 1\right] - 1 \tag{4.3.1}$$

where

$$A_1 = \frac{K_0(\Omega r_2) - K_0(\Omega r_1)}{A}, \quad A_2 = \frac{I_0(\Omega r_1) - I_0(\Omega r_2)}{A} \text{ and}$$

$$A = I_0(\Omega r_1)K_0(\Omega r_2) - I_0(\Omega r_2)K_0(\Omega r_1).$$

The volume flow rate q is given by

$$q = 2\int_{r_1}^{r_2} wr dr = 2\frac{(1+\lambda_1)}{\Omega^2}\frac{dp}{dz}A_3 - \left(r_2^2 - r_1^2\right) \tag{4.3.2}$$

in which

$$A_3 = \frac{A_1}{\Omega}\left[r_2 I_1(\Omega r_2) - r_1 I_1(\Omega r_1)\right] + \frac{A_2}{\Omega}\left[r_1 K_1(\Omega r_1) - r_2 K_1(\Omega r_2)\right] - \frac{\left(r_2^2 - r_1^2\right)}{2}.$$

From Eq. (4.3.3), we have

$$\frac{dp}{dz} = \frac{\left(q + \left(r_2^2 - r_1^2\right)\right)\Omega^2}{2A_3(1+\lambda_1)} \tag{4.3.3}$$

The pressure rise Δp per one wave length is given by

$$\Delta p = \int_0^1 \frac{dp}{dz} dz \tag{4.3.4}$$

Note that, as $M \to 0$ and $Da \to \infty$ our results coincide with the results of Hayat et al. (2006).

4.4. Results and Discussions

Fig. 4.2 shows the variation of axial pressure gradient $\frac{dp}{dx}$ with material parameter λ_1 for $\phi = 0.5,\ \varepsilon = 0.2,\ M = 1, Da = 0.1$ and $\overline{Q} = -1$. It is observed that, the axial pressure gradient $\frac{dp}{dx}$ decreases with increasing λ_1.

The variation of axial pressure gradient $\frac{dp}{dx}$ with Hartmann number M for $\phi = 0.5, \varepsilon = 0.2,\ \lambda_1 = 0.4$ and $\overline{Q} = -1$ is shown in Fig. 4.3. It is found that, the axial pressure gradient $\frac{dp}{dx}$ increases with increasing M.

Fig. 4.4 depicts the variation of axial pressure gradient $\frac{dp}{dx}$ with Darcy number Da for $\phi = 0.5,\ M = 1,\ \varepsilon = 0.2,\ \lambda_1 = 0.4$ and $\overline{Q} = -1$. It is found that, the axial pressure gradient $\frac{dp}{dx}$ decreases with an increase in Da.

The variation of axial pressure gradient $\frac{dp}{dx}$ with ε for $\phi = 0.5,\ \lambda_1 = 0.4,$ $M = 1,\ Da = 0.1$ and $\overline{Q} = -1$ is shown in Fig. 4.5. It is noted that, the axial pressure gradient $\frac{dp}{dx}$ increases with increasing ε.

Fig. 4.6 illustrates the variation of axial pressure gradient $\frac{dp}{dx}$ with ϕ for $\lambda_1 = 0.4,\ M = 1,\ \varepsilon = 0.2,\ Da = 0.1$ and $\overline{Q} = -1$. It is found that, the axial pressure gradient $\frac{dp}{dx}$ increases with increasing ϕ.

The variation of pressure rise Δp with time-averaged flux $\overline{Q}$ for different values of λ_1 with $\phi = 0.5,\ M = 1, \varepsilon = 0.2$ and $Da = 0.1$ is shown in Fig. 4.7. It is observed that, the time-averaged flux $\overline{Q}$ decreases with increasing λ_1 in the pumping region

$(\Delta p > 0)$, while it increases with increasing λ_1 in both the free-pumping $(\Delta p = 0)$ and co-pumping $(\Delta p < 0)$ regions. Further it is found that, the $\overline{Q}$ is more for Newtonian fluid $(\lambda_1 \to 0)$ than that of Newtonian fluid.

Fig. 4.8 shows the variation of pressure rise Δp with time-averaged flux $\overline{Q}$ for different values of M with $\phi = 0.5,\ M = 1, \varepsilon = 0.2$ and $Da = 0.1$. It is observed that, the time-averaged flux $\overline{Q}$ increases with increasing M in both the pumping and free-pumping regions, while it decreases with increasing M in the co-pumping regions.

The variation of pressure rise Δp with time-averaged flux $\overline{Q}$ for different values of Da with $\phi = 0.5,\ M = 1, \varepsilon = 0.2$ and $\lambda_1 = 0.3$ is shown in Fig. 4.9. It is noted that, the time-averaged flux $\overline{Q}$ decreases with increasing Da in both the pumping and free-pumping regions, while it increases with increasing Da in co-pumping region.

Fig. 4.10 depicts the variation of pressure rise Δp with time-averaged flux $\overline{Q}$ for different values of ε with $\phi = 0.5,\ M = 1, \lambda_1 = 0.4$ and $Da = 0.1$. It is found that, the time-averaged flux $\overline{Q}$ increases with increasing ε in the pumping region, while it decreases with increasing ε in both the free-pumping and co-pumping regions.

The variation of pressure rise Δp with time-averaged flux $\overline{Q}$ for different values of ϕ with $\lambda_1 = 0.4, M = 1,\ \varepsilon = 0.2$ and $Da = 0.1$ is depicted in Fig. 4.11. It is observed that, the time-averaged flux $\overline{Q}$ increases with increasing ϕ in the pumping region, while it decreases with increasing ϕ in both the free-pumping and co-pumping regions.

4.5. Conclusions

In this chapter, we modeled the peristaltic flow of a Jeffrey fluid through a porous in an annular region between two concentric tubes under the assumptions of low Reynolds number and long wavelength. The expressions for the velocity field and the pressure gradient are obtained analytically. It is found that, the axial pressure gradient and pumping decrease with increasing λ_1 and Da, whereas they increase with increasing M, ε and ϕ.

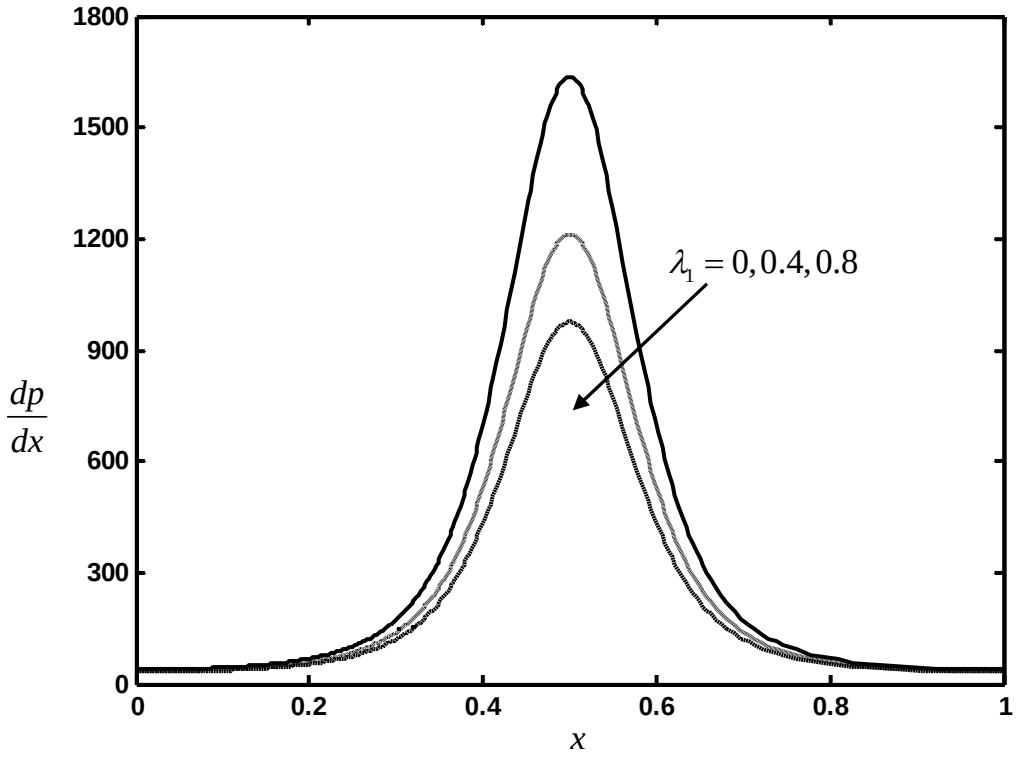

Fig. 4.2 The variation of axial pressure gradient $\frac{dp}{dx}$ with λ_1 for $\phi = 0.5$, $\varepsilon = 0.2$, $Da = 0.1$, $M = 1$ and $\overline{Q} = -1$.

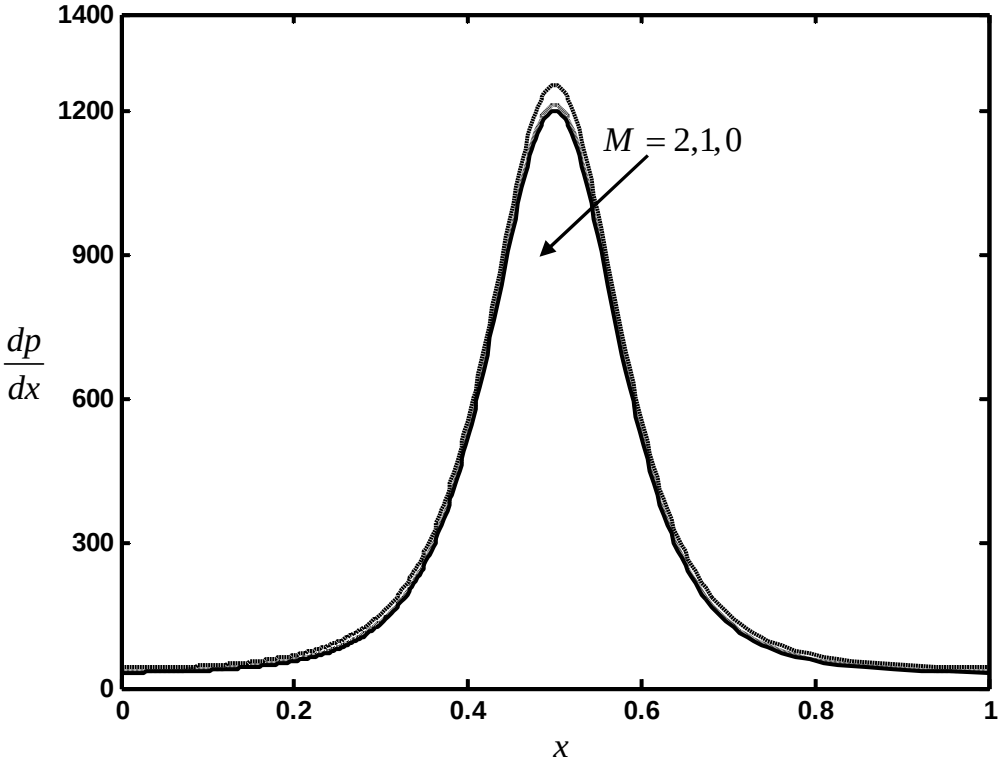

Fig. 4.3 The variation of axial pressure gradient $\frac{dp}{dx}$ with M for $\phi = 0.5$, $\varepsilon = 0.2$, $\lambda_1 = 0.4$, $Da = 0.1$ and $\overline{Q} = -1$.

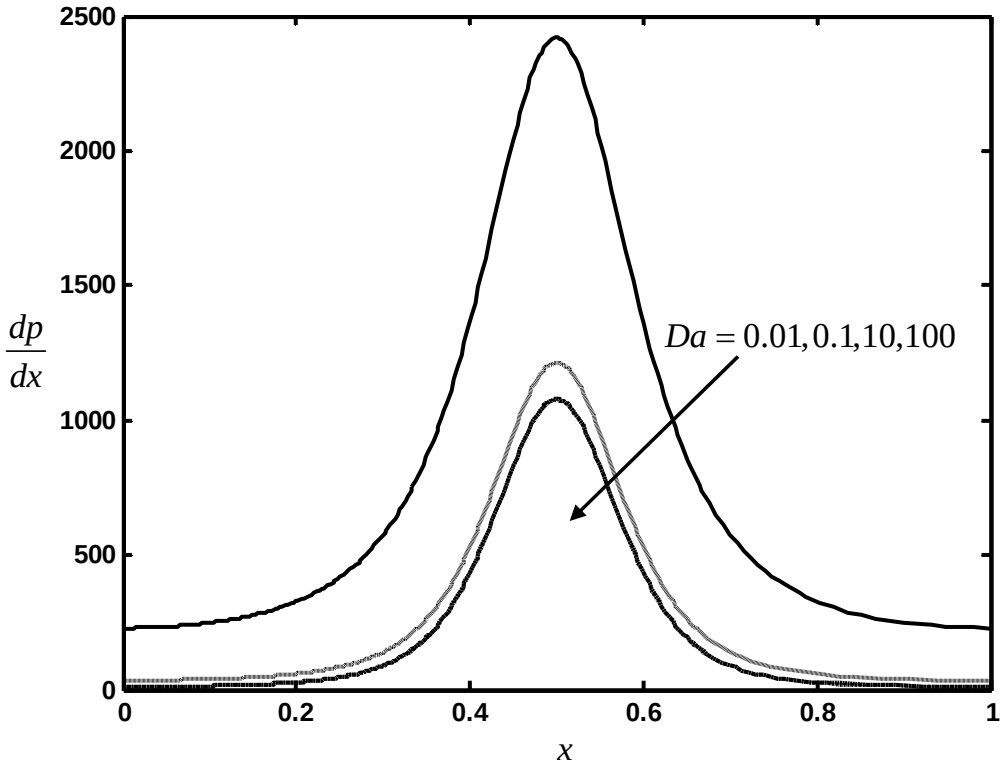

Fig. 4.4 The variation of axial pressure gradient $\frac{dp}{dx}$ with Da for $\phi = 0.5$, $\varepsilon = 0.2$, $\lambda_1 = 0.4$, $M = 1$ and $\overline{Q} = -1$.

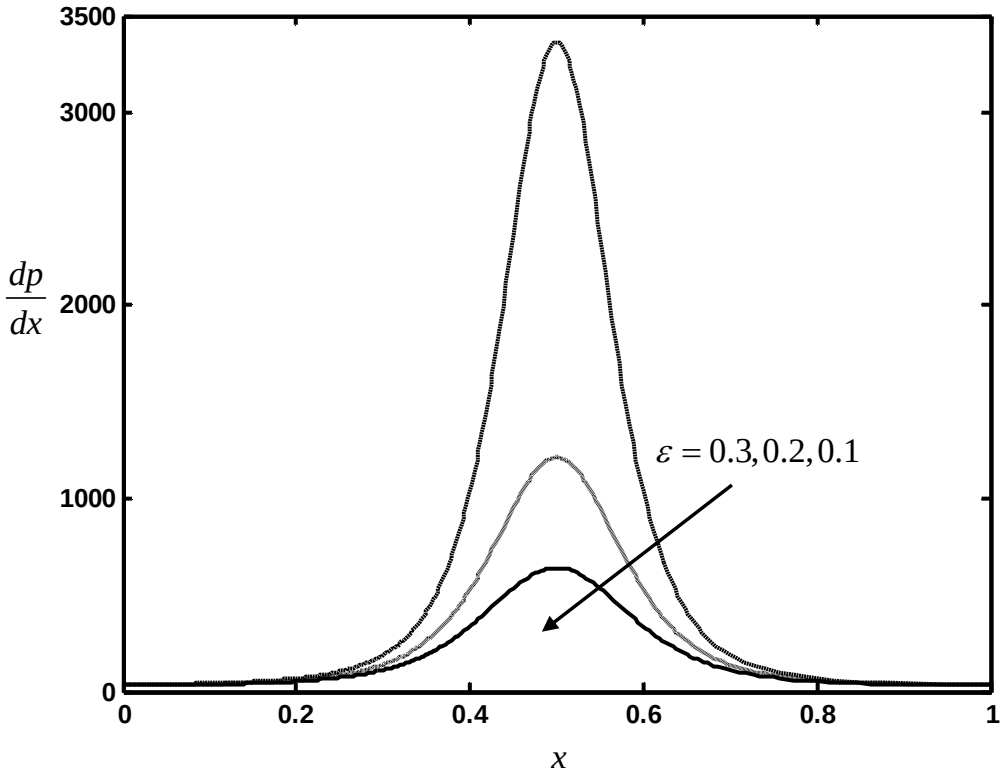

Fig. 4.5 The variation of axial pressure gradient $\frac{dp}{dx}$ with ε for $\phi = 0.5$, $\lambda_1 = 0.4$, $Da = 0.1$, $M = 1$ and $\overline{Q} = -1$.

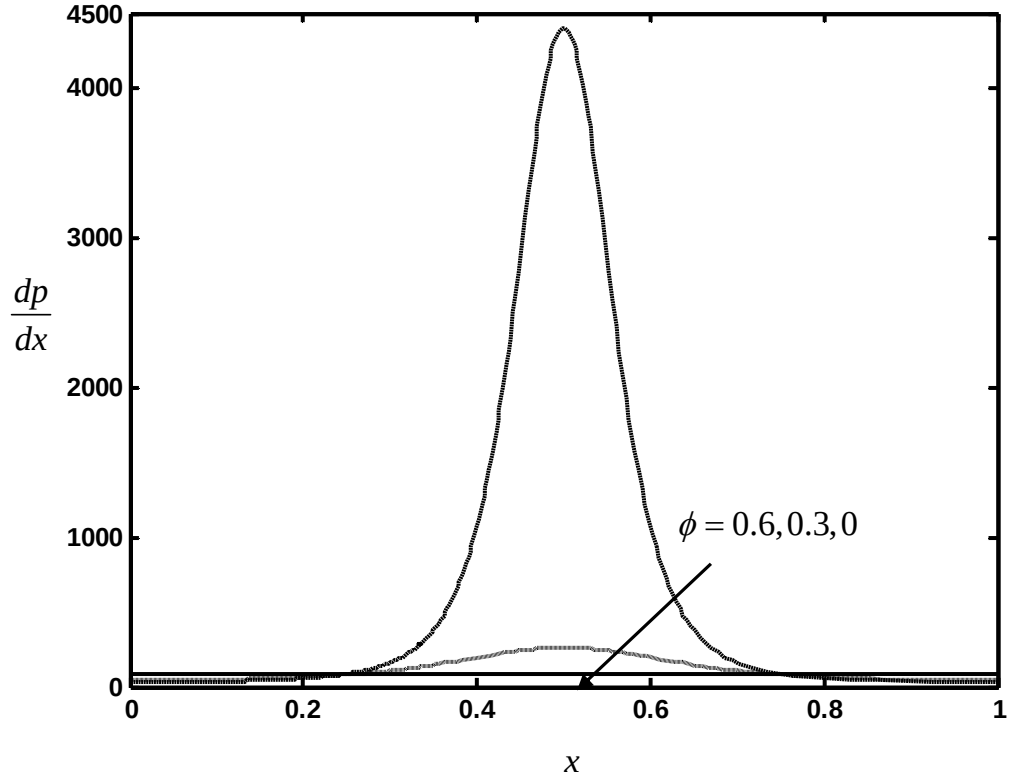

Fig. 4.6 The variation of axial pressure gradient $\frac{dp}{dx}$ with ϕ for $\lambda_1 = 0.4$, $\varepsilon = 0.2$, $Da = 0.1$, $M = 1$ and $\overline{Q} = -1$.

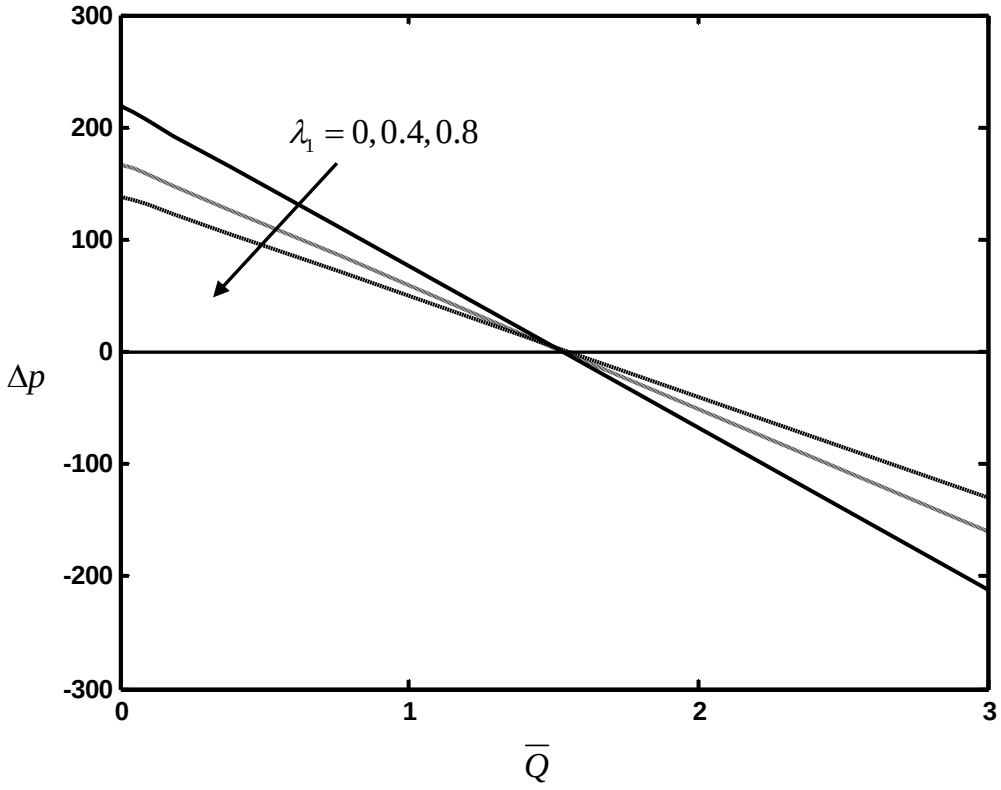

Fig. 4.7 The variation of pressure rise Δp with time averaged flux $\overline{Q}$ for different values of λ_1 with $\phi = 0.5,\ \varepsilon = 0.2$, $M = 1$ and $Da = 0.1$.

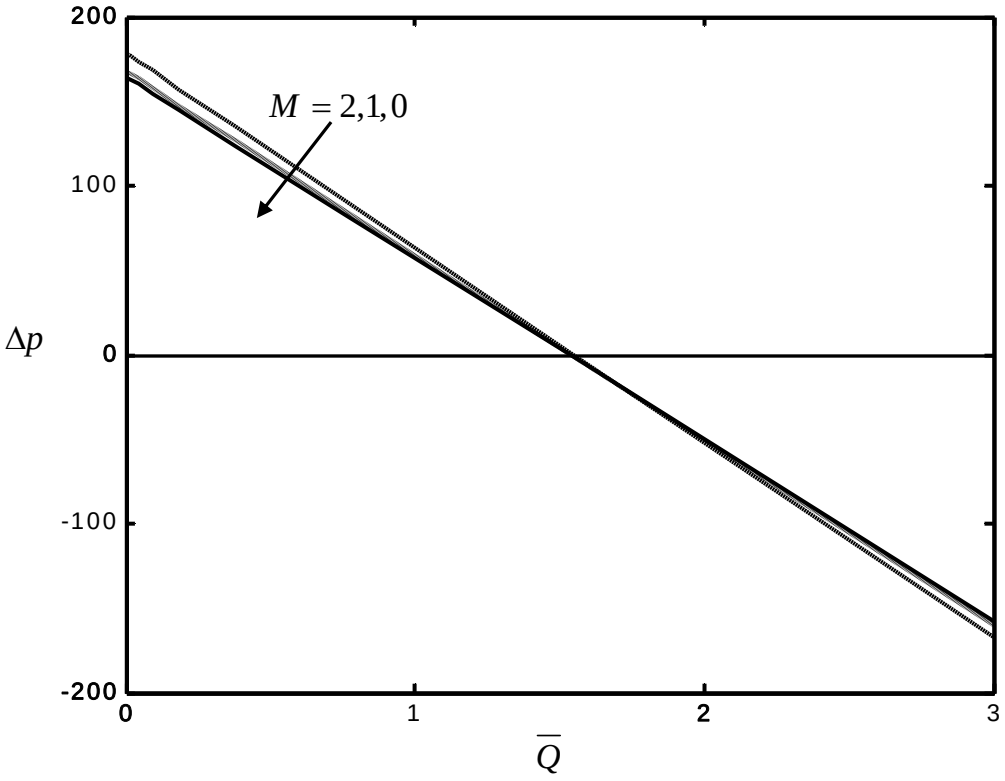

Fig. 4.8 The variation of pressure rise Δp with time averaged flux $\overline{Q}$ for different values of M with $\phi = 0.5,\ \varepsilon = 0.2$, $\lambda_1 = 0.4$ and $Da = 0.1$.

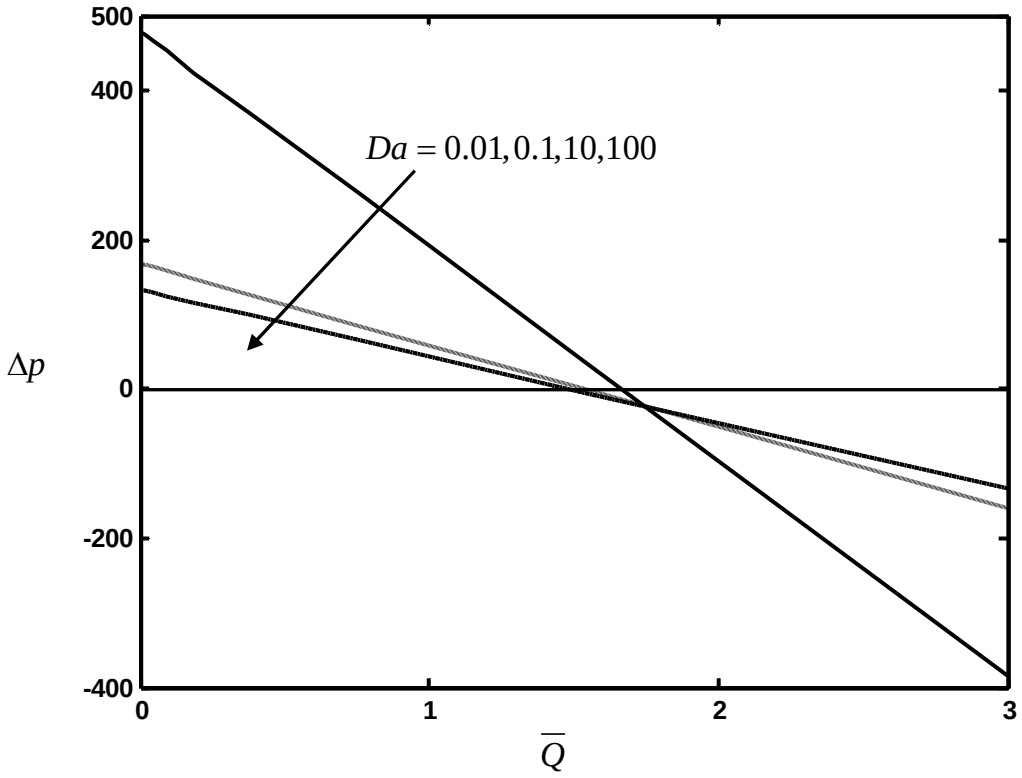

Fig. 4.9 The variation of pressure rise Δp with time averaged flux $\overline{Q}$ for different values of Da with $\phi = 0.5,\ \varepsilon = 0.2$, $M = 1$ and $\lambda_1 = 0.4$.

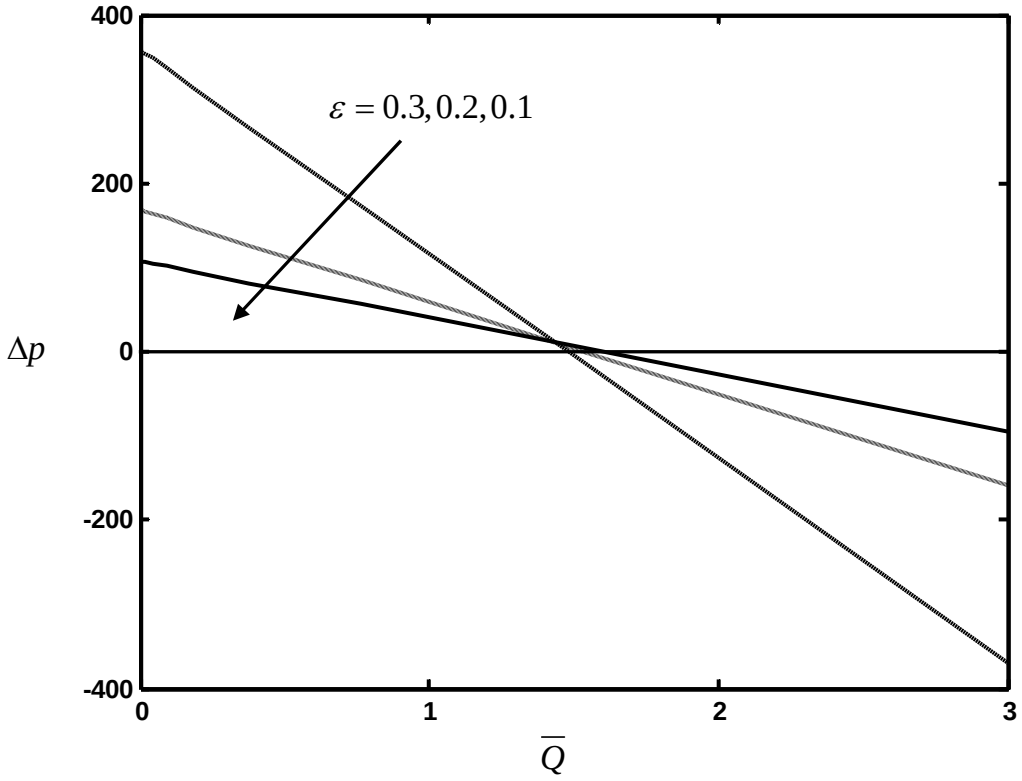

Fig. 4.10 The variation of pressure rise Δp with time averaged flux $\overline{Q}$ for different values of ε with $\phi = 0.5,\ \lambda_1 = 0.4$, $M = 1$ and $Da = 0.1$.

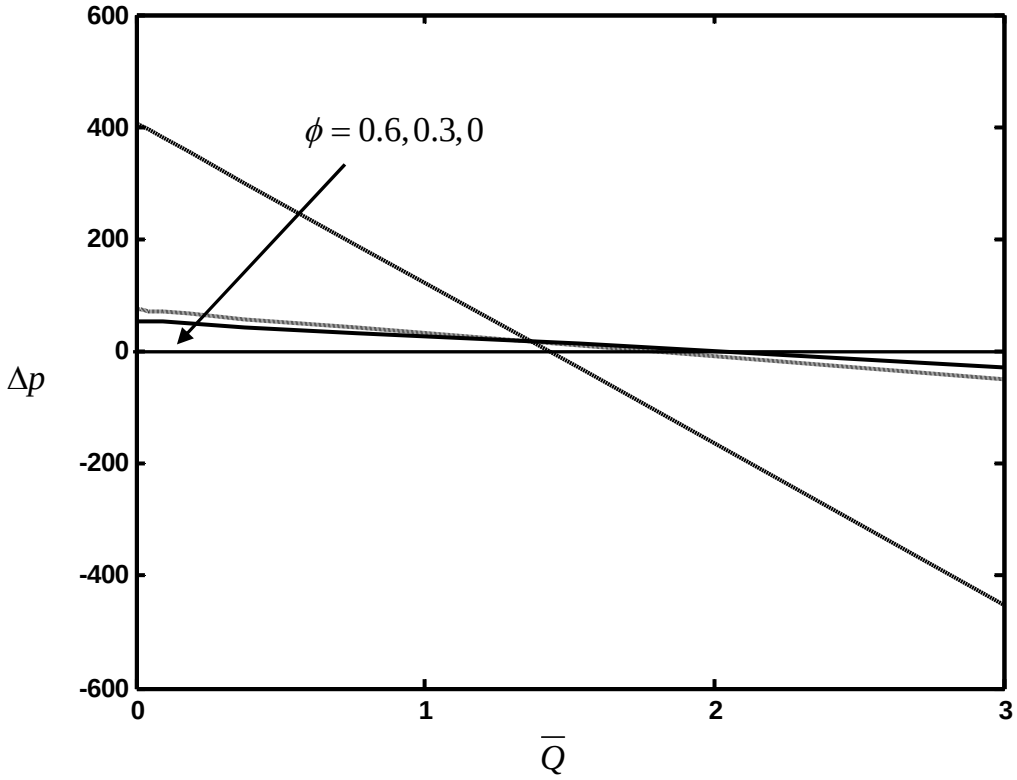

Fig. 4.11 The variation of pressure rise Δp with time averaged flux $\overline{Q}$ for different values of ϕ with $\lambda_1 = 0.4$, $\varepsilon = 0.2$, $M = 1$ and $Da = 0.1$.